

Optical Design and Fabrication of Fully Sputtered CdTe/CdS Solar Cells

To cite this article: R E Treharne *et al* 2011 *J. Phys.: Conf. Ser.* **286** 012038

View the [article online](#) for updates and enhancements.

Related content

- [Optical characterization of filtered vacuum arc deposited zinc oxide thin films](#)
E Çetinörgü, S Goldsmith, V N Zhitomirsky et al.
- [Electrodeposition and characterisation of ZnTe layers for application in CdTe based multi-layer graded bandgap solar cells](#)
D G Diso, F Fauzi, O K Echendu et al.
- [The dependence of filtered vacuum arc deposited ZnO–SnO₂ thin films](#)
E Çetinörgü, S Goldsmith, Z Barkay et al.

Recent citations

- [Excitation-dependent carrier lifetime and diffusion length in bulk CdTe determined by time-resolved optical pump-probe techniques](#)
Patrik Šajev *et al*
- [Plasmonic Sensor Based on Dielectric Nanoprisms](#)
Mahmoud H. Elshorbagy *et al*
- [Free Carrier Radiative Recombination and Photon Recycling in Lead Halide Perovskite Solar Cell Materials](#)
Yasuhiro Yamada *et al*

Optical Design and Fabrication of Fully Sputtered CdTe/CdS Solar Cells

R. E. Treharne, A. Seymour-Pierce, K. Durose

Department of Physics, Durham University, South Road, Durham. DH1 3LE

E-mail: r.e.treharne@durham.ac.uk

K. Hutchings, S. Roncallo, D. Lane

Department of Applied Science, Security and Resilience, Cranfield University,
Shrivenham, Swindon. SN6 8LA

Abstract. A model is presented for optimising the integrated intensity of light passing into the absorber layers of thin-film solar cells. Dispersion data for each of the transparent layers in the cells was obtained from variable angle spectroscopic ellipsometry. This data was then used in a transfer matrix model of multi-layer optics to determine the intensity spectrum passing over the interface from the transparent to the absorbing parts of the cell. Application of the method to the case of CdTe/CdS/ZnO/ITO/glass solar cells is described in detail, including the fitting of oscillator models to extract the complex dielectric function from the ellipsometry data. It was found that light coupling into the absorber was particularly sensitive to the CdS thickness but that tuning the ZnO (highly resistive transparent) layer was also influential. All-sputtered cells of this type were demonstrated as having efficiencies of 12.5% for $5 \times 5 \text{ mm}^2$ contacts.

1. Introduction

There are some significant opportunities to further increase the conversion efficiencies of thin-film solar cell devices; the present day best efficiencies are 16.5% for sublimation-grown [1] and 14.5% for sputtered [2] devices. These achievements fall short of the $\sim 30\%$ limit predicted for single junction devices. It is therefore likely that gains may be made, for example by optimising doping or by reducing the influence of polycrystallinity. It is the object of this paper to explore the *optical* gains in efficiency that may arise from optimising the thicknesses of both the window and transparent conducting oxide (TCO) layers of thin film solar cells. While the measurement and modelling methodology used in this work has general applicability, it is developed and tested here for the CdTe/CdS/ZnO/ITO/glass device as an exemplar. Industrially, SnO_2 is used as the transparent conductor, but here ITO (indium tin oxide) was chosen for its compatibility

with an in-house all-sputtered cell fabrication process. The CdS is n-type, and is a window layer admitting light into the p-type CdTe absorber. It is widely reported [1, 3, 4] that inclusion of a so-called ‘high resistive transparent’ (HRT) layer between the TCO and the window layer acts to enhance efficiency, although there is no consensus on the mechanism by which this occurs. In this work the HRT is ZnO.

Here, optical optimisation of the design of combined window and oxide multi-layers is investigated using the following methodology: Optical dispersion (or the refractive index and extinction coefficient) are obtained from ellipsometry [5, 6, 7]. This allows optimisation of the layer thicknesses, the results of which inform cell designs for experimental fabrication. In ellipsometry, the change in components of the reflected light are measured and related to the two standard ellipsometric parameters Ψ and Δ according to

$$\frac{R_p}{R_s} = \tan \Psi e^{i\Delta} \quad (1)$$

In the variant of this technique known as variable angle spectroscopic ellipsometry (VASE), both the angle and wavelength give additional experimental variables that contribute to the robustness of the data interpretation. The experimental spectra of Ψ and Δ are fitted using models of the complex frequency dependant dielectric function $\varepsilon(\omega)$. Physical models that are available to describe the dielectric function include:

- (a) Drude model [8]. Used for conductive materials in which there is a cut-off in transmission (i.e high reflectivity) in the near infra-red.
- (b) Lorentz oscillators [9, 10]. Appropriate for insulators and accounts for atom-dipole interactions.
- (c) PSEMI-M0 oscillators. Based on a model by Johs [11], and being appropriate for direct-gap semiconductors.

The usual procedure is to fit the measured spectra of Ψ and Δ by invoking appropriate oscillators. $\varepsilon(\omega)$ data obtained in this way gives the dispersion of both refractive index and of extinction coefficient (n and κ) directly. It is this data that is carried forward for modelling the optical transmission through multi-layer structures. The approach is to write the electromagnetic boundary conditions as simultaneous equations that are amenable to matrix algebra. This so-called ‘transfer matrix method’ allows the transmission and reflection spectra for multi-layers of thin films to be calculated and is described in detail in book-length reviews [12].

2. Experimental

Solar cells composed of a CdTe/CdS/ZnO/ITO/glass structure and samples of each of the individual layers were fabricated by radio-frequency sputtering. An AJA International Orion twin chamber system having 3” targets (obtained from Pi-Kem Ltd) was used, one chamber being dedicated to growth of the oxides and a vacuum transfer between the two being possible. The sputter targets were of the compounds themselves, with the ITO comprising 90% In₂O₃ and 10% SnO₂ by weight. All substrates were low iron soda-lime glass (Pilkington OptiWhiteTM).

Variable angle spectroscopic ellipsometry (VASE) was undertaken using a Woollam M2000UI instrument operating in reflection mode in the range 250-1500 nm, and at

angles of 50, 60 and 70°. Fitting of the spectra was achieved using the manufacturer's software. Transmission of the layers and stacks was measured using a Shimadzu Solid Spec UV-VIS-IR 3600 spectrophotometer. Transmission spectra were modelled using the transfer matrix method incorporating both dispersion of refractive index and extinction coefficient. Coding was done in FORTRAN95.

3. Results and Discussion

Ellipsometry data was obtained for each of the individual layers ITO, ZnO, CdS and CdTe. As an example, figure 1 shows the spectra of both Ψ and Δ (250-1500 nm) as function of angle. Fits obtained using appropriate oscillator models are shown as solid lines. For the ITO, which is considered to be highly conductive, it was necessary to use one Drude and two Lorentz oscillators. However, for the undoped ZnO, a single PSEMI-MO oscillator was sufficient, while both CdS and CdTe required two. Full details of the models chosen, and of the fitting procedures shall be presented elsewhere. The ITO fitting procedure generated a range of materials parameters that are compared to experimental and literature values in table 1. It is a confirmation of the model's validity that the thickness, carrier concentration and mobility, effective mass, band gap and permittivity all conform to the expected measured values.

Figure 2 shows the dispersion of n and κ in the wavelength range 250-1500 nm derived from the ellipsometry data for ITO, ZnO, CdS and CdTe. It is this data that was used in the transfer matrix model to simulate experimental transmission spectra for each of the individual layers in order to verify the procedure. Figure 3 shows examples of the simulated transmission spectra, and the corresponding experimental data. In figure 3a, a close correspondence is demonstrated for both ITO and for OptiWhite glass. Figure 3b shows how the modelling was able to predict the transmission spectrum of a test structure that was grown by sputtering and measured by spectrophotometry. The structure was CdS(120 nm)/ZnO(115 nm)/ITO(200 nm), with the experimental points

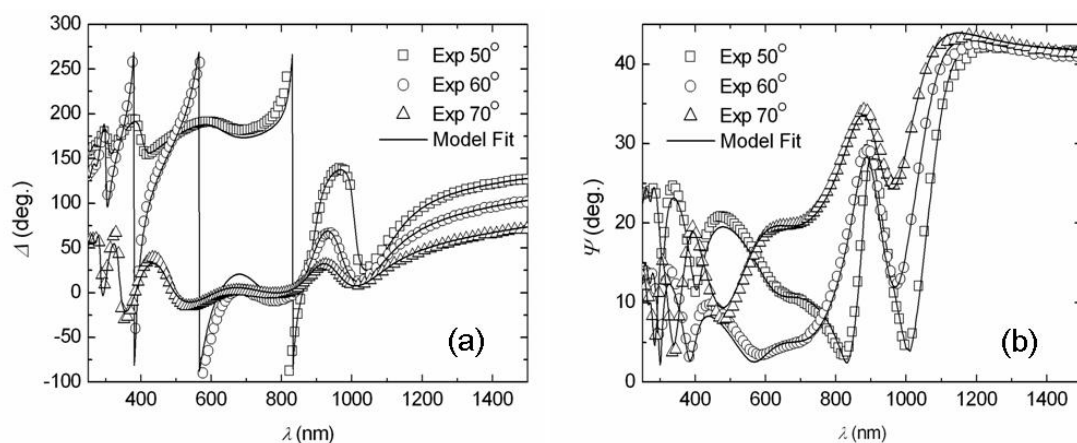


Figure 1. Experimental plots of a) Ψ and b) Δ of ITO film and the corresponding model fits

Table 1. Key parameters extracted from ellipsometric model for ITO and a comparison with measured or reference values.

	From Model	Comparison
d (nm)	237	230 ¹
n_e ($\times 10^{21}$ cm ⁻³)	1.3	1.2 ²
μ_e (cm ² V ⁻¹ s ⁻¹)	42	40 ²
m_e^*	0.4	0.35 [13]
E_G (eV)	4.1 ³	3.75-4.3 [14, 15]
ε_∞	3.0	3.95 [13]

¹ Surface profilometry measurement

² Hall measurement

³ Extrapolated from a $(h\nu\alpha)^2$ vs $h\nu$ plot

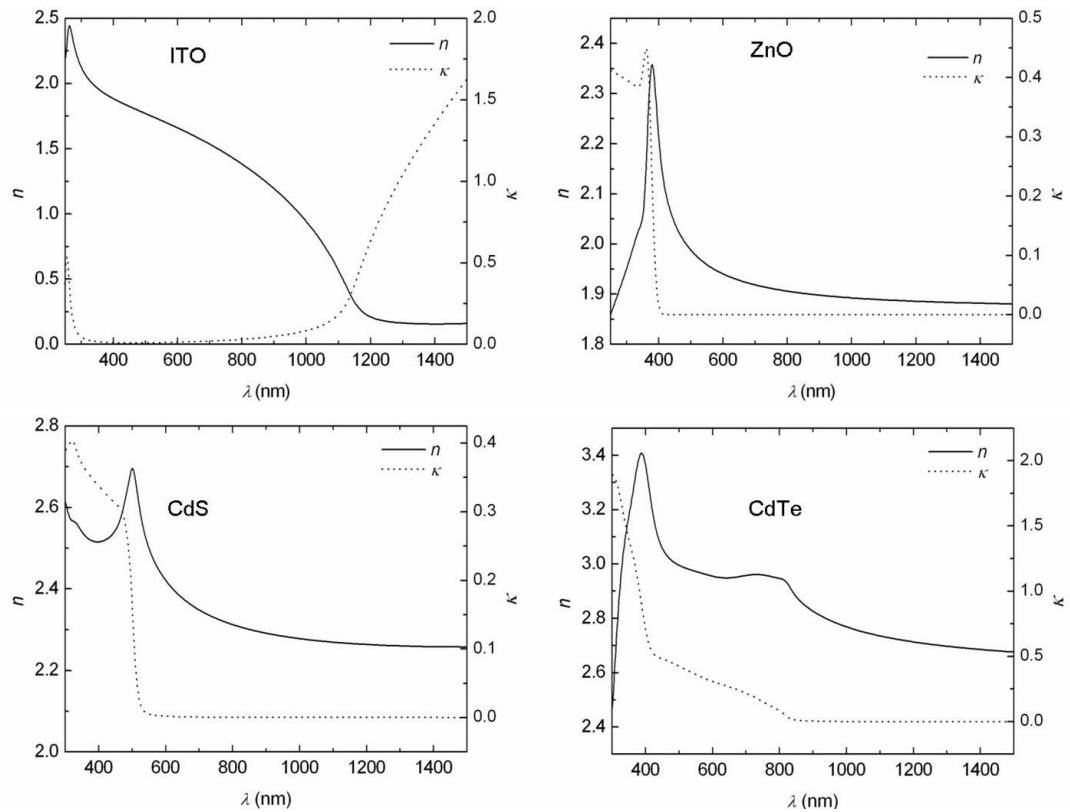


Figure 2. Extracted dispersion (n and κ) for ITO, ZnO, CdS and CdTe

in the figure conforming closely to the output from the model. Hence it was established with some confidence that the model is appropriate for use in estimating the transmission into the CdTe through the full CdS/ZnO/ITO/glass combination. The following results

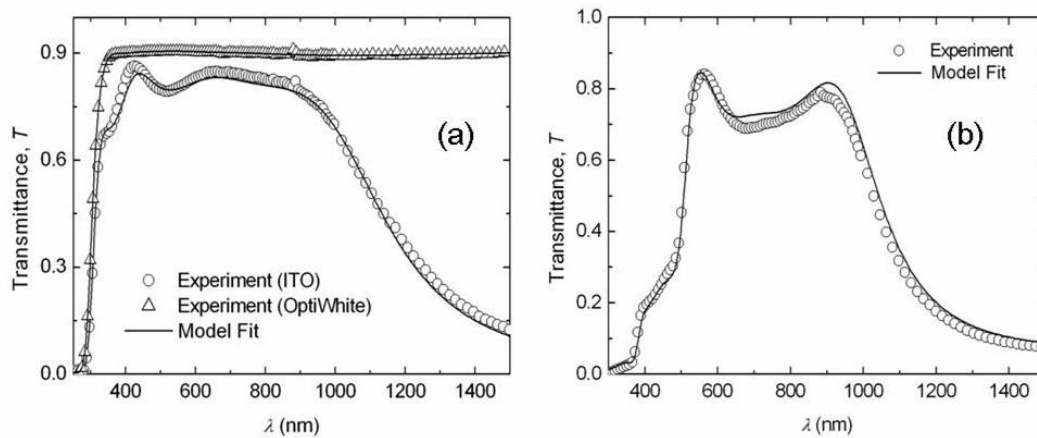


Figure 3. (a) Experimental transmission curves for ITO and OptiWhite substrate, and corresponding model fits. (b) Multi-layer model fit to the transmission curve for a CdS/ZnO/ITO/glass (200/115/120 nm) stack. Note that the exit medium in this case is air and not CdTe.

and discussion are for spectra calculated for light passing over the CdS-CdTe interface (whereas those in figure 3a assumed that transmission was into air rather than into CdTe). Note that the CdTe layer is assumed to have an infinite thickness (i.e all light is absorbed in this layer). A selection of the structures investigated are described in table 2. For each a full transmission spectrum was calculated, and from this the normalised integrated transmission into the CdTe absorber was evaluated as follows:

$$\tilde{T} = \frac{1}{b-a} \int_a^b T d\lambda \quad (2)$$

where \tilde{T} is the average fractional transmission over the range a-b specified. For CdTe/CdS devices, the range 300-850 nm was selected.

Table 2. A selection of ITO/ZnO/CdS stack structures showing the potential for increased transmittance in structures with thinner layers.

	d_{ITO} (nm)	d_{CdS} (nm)	d_{ZnO} (nm)	\tilde{T} (300-850 nm)	% change ¹
A	230	200	100	0.53	-
B	230	50	50	0.65	+22.6
C	115	50	50	0.67	+26.4
D	115	50	25	0.70	+32.1
E	115	25	25	0.71	+33.9
F	80	25	25	0.72	+35.3

¹ Relative to current baseline structure, A

Generally it was found that small changes in the thicknesses of CdS and ZnO had a greater influence on \tilde{T} than did changing the ITO thickness. This may be seen by comparing the baseline structure A to structure B (Table 2), in which the CdS and ZnO are thinned, which results in an increase in \tilde{T} of +22.6%. Thinning the ITO (C) causes a further +3.8% increase in transmission. Further reduction in the CdS and ZnO thickness (D and E) allow for further gains. This is explored further in figure 4, in which the ITO thickness is fixed at 115 nm and \tilde{T} is shown as a function of both the CdS and ZnO thicknesses. It is seen in the figure that changing the CdS thickness for a given ZnO thickness has a greater effect than *vice-versa*. For example, for a constant 50 nm of ZnO, reduction of the CdS from 200 to 50 nm increased \tilde{T} from 53 to 73%. However, for 50 nm of CdS, the same reduction in ZnO thickness acted to increase \tilde{T} from 64 to 72%. This behaviour may be accounted for by examining the transmission spectra in figure 5 in which the absorption loss in CdS (below ~ 500 nm) is revealed in the progression $F \rightarrow C \rightarrow A$. Nevertheless, reduction in the ZnO thickness has a significant effect on \tilde{T} , and by extension, possibly on cell efficiency. Overall, gains from optical optimisation of $> 30\%$ may be expected over the performance of the baseline structure A in table 2.

It must however be emphasised that these findings are based upon optical considerations only. The electrical impact of changing the layer thickness is not accounted for here - optical optimisation may well require different thicknesses than for electrical optimisation. Moreover, the materials data used in the modelling here was extracted from the layers in their as-grown state. Therefore the effects of processing, such as inter-diffusion, are not accounted for. In optimising solar cells, it is therefore essential to make real devices, and to use the results of this kind of optical study to inform the choice of layers and thicknesses for use in the experiments.

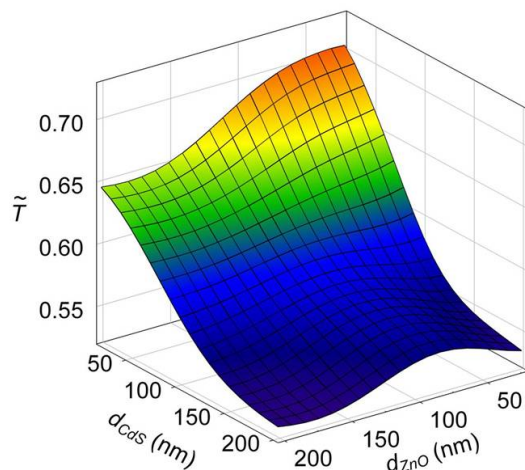


Figure 4. The variation in \tilde{T} shown as a function of both ITO and CdS thickness while maintaining a constant ITO thickness of 115 nm.

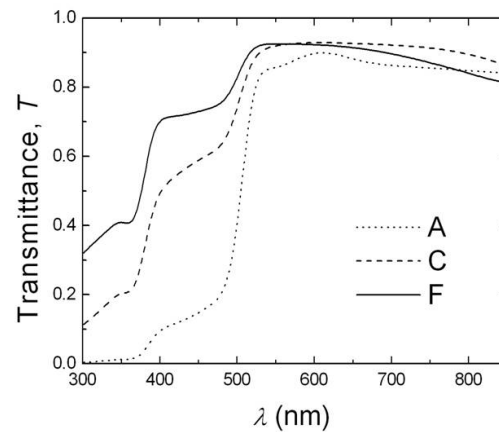


Figure 5. A selection of ITO/ZnO/CdS stack structures showing the potential for increased transmittance in structures with thinner layers.

Preliminary cells were therefore fabricated in preparation for the next stage of the investigation. The film thicknesses used were CdTe(3.4 μm)/CdS(200 nm)/ZnO(50 nm)/ITO(200 nm)/glass. Cells having $5 \times 5 \text{ cm}^2$ gold contacts were tested under AM1.5 spectral conditions at 1000 W.m^{-2} . The best working parameters obtained were V_{OC} (open circuit voltage) = 820 mV, J_{SC} (short circuit current density) = 24.9 mA.cm^{-2} and FF (fill factor) = 61% yielding an efficiency of 12.4%. This compares well with the best reported device of this kind (14.5%) [2], and hence provides the basis for continuing experiments. In further work a systematic study of varying the window and buffer layer design in real devices shall be undertaken, with the choices being informed by the results of the optical modelling.

4. Conclusions

Optical coupling into the absorber layers of thin film solar cells - after transmission through the TCO, high resistive transparent, and window layers - has been investigated. It was evaluated by a transfer matrix model that employed experimentally derived dispersion data for both the refractive indices and extinction coefficients of each material involved. The methodology was applied to cells comprising CdTe/CdS/ZnO/ITO, with dispersion data being extracted from as-grown sputtered films using variable angle spectroscopic ellipsometry. This involved modelling the dielectric dispersion using physical models that were appropriate for each layer, which then yielded optical dispersion data directly. Spectra for optical transmission into the absorber layer itself were derived for a series of test structures having systematically varied layer thicknesses. It was found that varying the ITO thickness had a relatively weak effect on optical transmission into the absorber, while the CdS and ZnO were more influential. The greatest effect was achieved by thinning the CdS to 25 nm, with gains of $\sim 20\%$ being possible with respect to a test structure with 100 nm thick CdS - this is expected from the blue absorption of CdS. Nevertheless, optical optimisation of the ZnO thickness may be expected to yield further gains of $\sim 5\%$.

Since the model is based on data for as-grown layers only, materials changes that occur during processing may be expected to influence the cell behaviour in practice. Moreover, optimisation based on optical criteria alone may compromise electrical performance. It is therefore essential to carry out optimisation of cells by experiment, using the results of this type of study as a starting point. Preliminary all-sputtered cells fabricated during this work achieved a maximum efficiency of 12.5%, this being an excellent starting point for optically informed device optimisation.

Acknowledgements

The authors would like to thank Neil McSporran and Paul Warren of Pilkington for useful discussions. They are also grateful to Michelle Sestak of Toledo University for helpful discussion on ellipsometry. Funding for the PV-21 project was provided by the EPSRC SUPERGEN programme.

References

- [1] Wu X, Keane J C, Dhare R G, DeHart C, Albin D S, Dudam A, Gessert T A, Asher S, Levi D H and Sheldon P 2001 *Proc. 17th Eur. PVSEC (Munich)* 995

- [2] Gupta A and Compaan A 2004 *App. Phys. Lett.* **85** 684
- [3] Bosio A, Romeo N, Mazzamuto S and Canevari V 2006 *Prog. Cryst. Growth Charact. Mater.* **52** 247
- [4] Ferekides C S, Marinskiy D, Viswanathan V, Tetali B, Palekis V, Selvaraj P and Morel D L 2000 *Thin Solid Films* **361** 520
- [5] Durose K, Asher S, Jaegermann W, Levi D, McCandless B, Metzger W, Moutinho H, Paulson P, Perkins C, Sites J, Teeter G and Terheggen M 2004 *Prog. Photovoltaics: Res. App.* **12** 177
- [6] Paulson P and Mathew X 2004 *Sol. Energ. Mat. Sol. Cells* **82** 279
- [7] Li J, Podraza N and Collins R 2008 *Phys. Stat. Sol. A* **205** 901
- [8] Edwards P P, Porch A, Jones M O, Morgan D V and Perks R M 2004 *Dalt. Trans.* 2995
- [9] Synowicki R 1998 *Thin Solid Films* **313** 394
- [10] Jung Y 2004 *Thin Solid Films* **467** 36
- [11] Johs B, Herzinger C, Dinan J, Cornfeld A and Benson J 1998 *Thin Solid Films* **313** 137
- [12] Macleod H A 1986 *Thin-film Optical Filters* (Bristol: Adam Hilger Ltd)
- [13] Hamberg I and Granqvist C 1986 *J. Appl. Phys.* **60** R123
- [14] George J and Menon C 2000 *Surf. Coat. Tech.* **132** 45
- [15] Terzini E, Thilakan P and Minarini C 2000 *Materials Science and Engineering B* **77** 110